^{203,205}Tl NMR studies of Crystallographically Characterized Thallium Alkoxides. X-ray Structures of $[Tl(OCH_2C(CH_3)_3)]_4$ and $[Tl(OAr)]_\infty$ where OAr = $OC_6H_3(Me)_2$-2,6 and $OC_6H_3(Pr^i)_2$-2,6

Cecilia A. Zechmann, Timothy J. Boyle*, Dawn M. Pedrotty
Sandia National Laboratories, Advanced Materials Laboratory, 1001 University Boulevard, S.E., Albuquerque, New Mexico 87106

Todd M. Alam, David P. Lang
Sandia National Laboratories, Department of Organic Materials, P.O. Box 5800, Albuquerque, New Mexico, 87185-1407.

Brian L. Scott
Los Alamos National Laboratories, CST-18, Chemical Science and Technology Division - X-ray Diffraction Laboratory, Los Alamos, New Mexico 87545

*Author to whom correspondences should be sent.

DISCLAIMER

Abstract. $[Tl(OCH_2CH_3)]_4$, (**1**) was reacted with excess HOR to prepare a series of $[Tl(OR)]_n$ where OR = $OCHMe_2$ (**2**, n = 4), $OCMe_3$ (**3**, n = 4), OCH_2CMe_3 (**4**, n = 4), $OC_6H_3(Me)_2$-2,6 (**5**, n = ∞), and $OC_6H_3(Pr^i)_2$-2,6 (**6**, n = ∞). Single crystal X-ray diffraction was used to determine the structure of compounds ligated by more sterically demanding ligands. Compound **4** was found to adopt a cubane structure, while **5** and **6** formed linear polymeric structures. These compounds were additionally characterized by $^{203,205}Tl$ solution and ^{205}Tl solid state NMR. Compounds **1 – 4** were found to remain intact in solution while the polymeric species, **5** and **6**, appeared to be fluxional. While variations in the solution and solid state structures for the tetrameric $[Tl(OR)]_4$ and polymeric $[Tl(OAr)]_\infty$ may be influenced by the steric hindrance of their respective ligands, the covalency of the species is believed to be more an effect of the parent alcohol acidity.

Introduction

Metathesis reactions are commonly used to generate complex metal alkoxides and typically employ alkali metal alkoxide precursors (AOR where A = Li, Na, K [1-5] For example, in the titanium system, the parent alkoxide ($Ti(OR)_4$) is reacted with AOR to generate the heterometallic species (eq 1),[6-9] $[ATi(OR)_5]_n$ (n = 2 or ∞ depending upon the ligand set). These double alkoxides can then be used in a metathetical manner to generate complex compounds (eq 2).[6-9] Unfortunately, these reactions are often complicated since the "$Ti(OR)_5^-$" anion does not always cleanly transfer, resulting in halide or alkali metal retention.[8,9] Previously, we have investigated the solid state structures of the "$ATi(OR)_5$" and found the arrangement of the cations limits the accessibility of the alkali metal cation.

$$n\,Ti(OR)_4 + n\,AOR \rightarrow [ATi(OR)_5]_n \qquad n = 2 \text{ or } \infty \qquad (1)$$

$$[ATi(OR)_5]_n + n\,MCl_x \rightarrow [MTi(OR)_5Cl_{x-1}]_n + n\,ACl \qquad (2)$$

One alternative metathesizable metal that has been understudied for these types of reactions is thallium.[10,11] This is especially surprising as thallium alkoxides ($[Tl(OR)]_n$) were known as early as the mid 1800's (first prepared by Lamy[12]) and the structural aspects of several were determined by spectroscopic methods.[13,14]

It is important to fully understand the structural aspects of the "simple" precursors to exploit them in a metathetical synthetic approach. Therefore, we have characterized a series of $[Tl(OR)]_n$, including OR = $OCHMe_2$ (OPr^i, **2**, n = 4), $OCMe_3$ (OBu^t, **3**, n = 4), OCH_2CMe_3 (ONep, **4**, n = 4), $OC_6H_3(Me)_2$-2,6 (DMP, **5**, n = ∞), and $OC_6H_3(Pr^i)_2$-2,6 (DIP, **6**, n = ∞), using ^1H, ^{13}C, and $^{203,205}Tl$ NMR spectroscopy, and X-ray crystallography when possible. Details of the synthesis and characterization of these compounds are discussed below.

Experimental

All compounds described below were handled with rigorous exclusion of air and water using standard Schlenk line and glove box techniques. FT-IR data was obtained on a Bruker Vector 22 using KBr pellets under an atmosphere of flowing nitrogen. TGA/DTA experiments were performed on a Polymer Laboratories STA 1500 Instrument under an atmosphere of flowing oxygen up to 650 °C at a ramp rate of 5 °C/ min. Elemental analyses were performed on a Perkin-Elmer 2400 CHN-S/O Elemental Analyzer.

For the solid state NMR investigations, each sample was prepared from dried crystalline material that was handled and stored under an argon atmosphere. All $^{13}C\{^{1}H\}$ solid state MAS NMR spectra were obtained on an AMX400 spectrometer at a frequency of 100.6 MHz using a 4 mm bb MAS probe, spinning at 4 kHz. A standard single pulse Bloch decay, 64-128 scan averages, 2 sec recycle delay and a 2 μs pulse were used for all experiments. The ^{205}Tl spectra were referenced to solid $Tl(NO_3)$ ($\delta = 0.0$ ppm)

For solution spectra, each dried crystalline sample was redissolved in an appropriate dueterated solvent at saturated solution concentrations and sealed under vacuum. All solution spectra were obtained on a DMX400 spectrometer at 399.9 and 100.5 MHz for ^{1}H and $^{13}C\{^{1}H\}$ experiments, respectively. A 5 mm bb probe was used for all experiments. ^{1}H NMR spectra were obtained using a direct single pulse excitation with a 10 s recycle delay. $^{13}C\{^{1}H\}$ NMR spectra were obtained using composite pulse ^{1}H decoupling with a 5 sec recycle delay and a $\pi/4$ pulse excitation. High resolution solution $^{203,205}Tl$ NMR spectra were obtained on a Bruker DMX400 at 231.0 and 228.9 MHz for ^{205}Tl and ^{203}Tl, respectively. All spectra were obtained on a specially tuned 5 mm $Tl\{^{1}H\}$ probe, using single pulse excitation and a 1 sec recycle delay. Both the ^{203}Tl and ^{205}Tl spectra were referenced to 0.001M $Tl(NO_3)$ in D_2O ($\delta = 0.0$ ppm).

Simulations of the multiplet patterns in the ^{203,205}Tl high resolution spectra were obtained using the simulation component in the NMR Utility Transform Software (NUTS) program (Acorn NMR, Fremont, CA). The simulation program was modified to include both the ^{205}Tl and ^{203}Tl spin 1/2 nuclei along with the relative natural abundance of these two nuclei, 79.5 % and 29.5 % respectively. Additional information regarding the ^{203,205}Tl NMR simulations can be found in the supporting material.

Iso-propanol (HOPr^{i}) and all solvents were freshly distilled from the appropriate drying agent and stored over molecular sieves. *Tert*-butanol (HOBu^{t}) was dissolved in hexanes (1.7M solution) and stored over molecular sieves for a minimum of 24 hr. prior to use. The following compounds were stored under argon upon receipt (Aldrich) and used without further purification: neo-pentanol (HONep), 2,6-di-methylphenol (H-DMP), 2,6-di-isopropylphenol (H-DIP), and thallium ethoxide, **1**. Since **2** - **6** were all prepared in a similar manner, a general synthetic route is described below with any variations noted in the individual sections.

General Synthesis. $[TlOEt]_4$, **1**, was added to a solution comprised of a large excess of the appropriate alcohol (HOR) dissolved in toluene. The resulting mixture was stirred overnight at room temperature, followed by warming in a water bath (~50°C) for two hours. The solvent was then removed *in vacuo* with heating to facilitate the removal of any remaining volatile material. The resulting solid was redissolved in hexanes (**2–4**), toluene (**5**), or THF (**6**). Any insoluble component was removed by centrifugation and the final product isolated by removal of the solvent *in vacuo*. Crystalline products were isolated by either slow evaporation of solvent or slow cooling of a saturated hot solution.

[Tl(OPr^i)]$_4$ (2). Used HOPr^i (10 mL, 130 mmol) in toluene (10 mL) and **1** (1.0 mL, 3.5 mmol) in toluene (5 mL). Isolated yield 2.9 g (78%). FT-IR (KBr, cm^{-1}) 2947(s), 2913(m), 2852(w), 2803(w), 2779(w), 2765(w), 2750(w), 2598(w), 2588(w), 1450(m), 1368(m), 1355(m), 1327(m), 1156(w), 1114(s), 948(s), 810(m), 511(m), 466(m). ^{1}H NMR (399.9 MHz, C_6D_6, 20°C) δ 5.16 (1H, sept, OC*H*(CH$_3$)$_2$, $^3J_{H\text{-}H}$ = 6 Hz), 1.33 (6H, d, OCH(C*H*$_3$)$_2$, $^3J_{H\text{-}H}$ = 6 Hz. ^{13}C{^{1}H} NMR (100.1 MHz, toluene-d_8) δ 66.2 (O*C*H(CH$_3$)$_2$), 29.1 (OCH(*C*H$_3$)$_2$). ^{205}Tl NMR (231.0 MHz, toluene-d_8) δ 3067 (sept, $^2J_{205\text{-}203}$ = 2.57 kHz). ^{203}Tl NMR (228.9 MHz, toluene-d_8) δ 3067 (sept, $^2J_{205\text{-}203}$ = 2.57 kHz). TGA (oxygen): Total wt loss (%) Found (Calculated for Tl_2O_3): 11.5 (10.0). DTA: Exotherm at 210 °C. Anal. Calc. for C_3H_7OTl: C, 13.68%; H, 2.68 %. Found: C, 12.98 %; H, 2.53 %.

[Tl(OBu^t)]$_4$ (3). Used HOBu^t (10 mL, 105 mmol) in toluene (5 mL) and **1** (0.58 mL, 2.1 mmol) in toluene (5 mL). Yield 2.02g (89%). FT-IR (KBr, cm^{-1}) 2948(s), 2916(m), 2886(m), 2853(m), 1456(m), 1376(s), 1353(s), 1215(m), 1173(s), 915(s) 745(m), 499(s), 440(w). ^{1}H NMR (399.9 MHz, toluene-d_8) 1.41 ppm (s, OC(C*H*$_3$)$_3$). ^{13}C{^{1}H} NMR (100.1 MHz, toluene-d_8) δ 71.7 (O*C*(CH$_3$)$_3$), 33.6 (OC(*C*H$_3$)$_3$). ^{205}Tl NMR (231.0 MHz, toluene-d_8) δ 3285 (sept, $^2J_{205\text{-}203}$ = 2.25 kHz). ^{203}Tl NMR (228.9 MHz, toluene-d_8) δ 3285 (sept, $^2J_{205\text{-}203}$ = 2.25 kHz). TGA (oxygen): Total wt. loss (%) Found (Calculated for Tl_2O_3): 16.3 (17.7). DTA: small exotherms at 241°C and 272°C. Anal. Calc. for $C_4H_{11}OTl$: C, 17.19 %; H, 3.97 %. Found: C, 16.31 %; H, 2.92 %.

[Tl(ONep)]$_4$ (4). Used HONep (2.6 g, 29 mmol) in toluene (10 mL) and **1** (0.5 mL, 1.8 mmol). Isolated yield: 1.9 g (92%). X-ray quality crystals could be obtained by slow evaporation (room-temperature) of a saturated hexanes or toluene solution. FT-IR (KBr, cm^{-1}) 2947(s), 2893(m), 2858(m), 2793(m), 2771(m), 2737(w), 2684(m), 1473(m), 1393(m), 1357(m), 1250(w), 1210(w), 1044(s), 1010(s), 930(w), 892(w), 544(m), 415(w). ^{1}H NMR (399.9 MHz,

toluene-d_8) δ 3.61 (2H, s, OCH_2CMe_3), 1.00 (9H, s, OCH_2CMe_3). $^{13}C\{^1H\}$ NMR (100.1 MHz, toluene-d_8) δ 76.9 (OCH_2CMe_3), 33.8 (OCH_2CMe_3), 27.3 (OCH_2CMe_3). ^{205}Tl NMR (231.0 MHz, toluene-d_8) δ 2561 (sept, $^2J_{205\text{-}203}$ = 2.58 kHz). ^{203}Tl NMR (228.9 MHz, toluene-d_8) δ 2562 (sept, $^2J_{205\text{-}203}$ = 2.58 kHz). TGA (oxygen): Total wt. loss (%) Found (Calculated for Tl_2O_3): 21.0 (21.7). DTA: large exotherm at 205°C. Anal Calc. for $C_{20}H_{44}O_4Tl_4$: 20.60, C%; 3.80, H%. Found: 20.52, C%; 3.63, H%.

[Tl(DMP)]$_\infty$ (5). Used H-DMP (1.24 g, 10.6 mmol) in toluene (12 mL) and **1** (0.70 mL, 2.7 mmol). Crystalline yield: 2.88 g (89%). X-ray quality crystals were obtained upon the cooling of saturated hot toluene or THF solutions. FT-IR (KBr, cm^{-1}) 2998(w), 2961(m), 2922(m), 2906(m), 2840(w), 1581(s), 1457(s), 1410(s), 1367(m), 1318(w), 1262(s), 1231(s), 1158(w), 1086(s), 978(w), 946(w), 910(w), 838(s), 761(s), 681(m), 501(m). ^1H NMR (399.9 MHz, toluene-d_8) δ 7.16 (2H, d, $OC_6H_3(CH_3)_2$, $^3J_{H\text{-}H}$ = 7.2 Hz), 6.63 (1H, t, $OC_6H_3(CH_3)_2$, $^3J_{H\text{-}H}$ = 7.2 Hz), 2.48 (6H, s, $OC_6H_3(CH_3)_2$). $^{13}C\{^1H\}$ NMR (100.1 MHz, toluene-d_8) δ 128.8, 128.3, 127.9, 127.6, $OC_6H_3(CH_3)_2$), 16.9 ($OC_6H_3(CH_3)_2$). ^{205}Tl NMR (231.0 MHz, toluene-d_8) δ 1989 (s). ^{203}Tl NMR (228.9 MHz, toluene-d_8) δ 1989 (s). TGA (oxygen): Total wt. loss (%) Found (Calculated for Tl_2O_3): 29.9 (32.5). DTA: large exotherm at 391°C. Anal Calc. for C_8H_9OTl: C, 29.52%; H, 2.79%. Found: C, 30.03%; H, 3.06%.

[Tl(DIP)]$_\infty$ (6). Used H-DIP (3.00 g, 16.8 mmol) in THF (100 mL) and **1** (0.95 mL, 3.4 mmol). Crystalline yield: 3.66 g (71%). X-ray quality crystals were obtained by the slow cooling of hot, saturated THF or pyridine solutions. FT-IR (KBr, cm^{-1}) 2952(s), 2919(m), 2863(m), 1581(m), 1457(m), 1418(s), 1356(m), 1324(s), 1253(s), 1200(m), 1156(m), 1096(m), 1037(w), 883(w), 833(s), 797(w), 762(s), 676(m), 524(m), 446(w), 421(w). ^1H NMR (399.9 MHz, THF-d_8) δ 6.94 (2H, d, $OC_6H_3(CH(Me)_2)_2$, $^3J_{H\text{-}H}$ = 7.6 MHz), 6.42 (1H, t,

$OC_6H_3(CH(Me)_2)_2$, $^3J_{H-H}$ = 7.6 MHz), 3.87 (2H, sept, $OC_6H_3(CH(CH_3)_2)_2$, $^3J_{H-H}$ = 6.8 MHz), 1.04 (12H, d, $OC_6H_3(CH(CH_3)_2)_2$, $^3J_{H-H}$ = 6.8 MHz). $^{13}C\{^1H\}$ NMR (100.1 MHz, THF-d_8) δ 159.1, 138.3, 123.1, 116.8 ($OC_6H_3(CH(CH_3)_2)_2$), 27.4 ($OC_6H_3(CH(CH_3)_2)_2$), 26.1($OC_6H_3(CH(CH_3)_2)_2$). ^{205}Tl NMR (231.0 MHz, THF-d_8) δ 1840 (s). ^{203}Tl NMR (228.9 MHz, d_8-THF) δ 1840 ppm (s). TGA (oxygen): Total wt. loss (%) Found (Calculated for Tl_2O_3): 43.7 (40.2). DTA: large exotherm at 412°C (recoalescence peak). Anal Calc. for $C_{24}H_{34}OTl$: 37.77, C%; 4.49, H%. Found: C, 37.83, C%; 4.48, H%.

Structure Determinations. For each sample, a suitable crystal was mounted from a pool of Fluorolube™ HO-125 onto a thin glass fiber and then immediately placed under a liquid N_2 stream on a Bruker AXS diffractometer. Data collection parameters for all compounds are given in Table 1. The radiation used was graphite monochromatized Mo Kα radiation (λ= 0.71073 Å). Lattice determination and data collection were carried out using SMART Version 5.054 software.[15] Data reduction was performed using SAINT+ 5.02 software.[16] Absorption correction using SADABS[17] in SHELXTL 5.1[18] was carried out for all compounds. Structure solution, graphics, and preparation of publication materials were performed using SHELXTL. After all non-hydrogen atoms were identified, the hydrogen atoms were fixed in positions of ideal geometry and the entire structure refined within the XSHELL[19] software. These idealized hydrogen atoms had their isotropic temperature factors fixed at 1.2 or 1.5 times the equivalent isotropic U of the C atoms to which they were bonded. Individual differences in data collection, structure solution, and refinement are reported below.

The structure of **4** was solved in space group P-43n using Direct methods and difference Fourier techniques. The initial solution revealed the Tl and O atom positions. There were two

independent molecules per unit cell with one molecule on a site of 23 symmetry and the other on a site of –4 symmetry. In the former molecule the ONep group was disordered on a site of 3-fold rotation symmetry. The ONep group of the molecule occupying the –4 symmetry element was also severely disordered. Both of these ONep groups were modeled as rigid bodies. The modeling of the ONep groups in this fashion resulted in a drop of about 3% in R1. There were still several large temperature factors on some carbon atoms, but additional attempts to model the disorder were not successful. Due to the disorder of the ONep groups, hydrogen atom positions were not considered in the model. The final refinement[20] converged to R1= 0.0682 and $R2_w$= 0.2015, with isotropic temperature factors on all atoms except thallium. Structure solutions and refinements of **5** and **6** were straightforward. Additional details of data collection and structure refinement are listed in Table 1.

Results and Discussion.

Synthesis. The $[Tl(OR)]_n$ investigated were synthesized by an alcohol (HOR) exchange reaction involving the commercially available **1** and the appropriate HOR (eq 3). The complete exchange was insured through the addition of an excess of HOR and by heating the reaction. The evolved EtOH and any excess HOR were removed *in vacuo*, assisted with mild heating or by filtration, yielding a white solid. For **2** and **3** a small amount of decomposition (formation of a black powder thought to be Tl°) was noted upon warming; however, compounds **4** - **6** were more stable and no discoloration was observed during the synthesis or drying of these compounds.

$$[Tl(OEt)]_4 + (xs)\ HOR \rightarrow [Tl(OR)]_n + 4\ HOEt \qquad (3)$$

The IR stretches associated with the individual ligands were present in each sample with the expected loss of the O-H stretch (typically observed as a broad resonance > 3000 cm^{-1}). The asymmetric Tl-O stretches of **2** - **4** were observed in the FT-IR at frequencies ≤ 500 (cm^{-1}). The Tl-(μ-O) stretch of **5** and **6** were identified at 501 and 524 cm^{-1} respectively.

During the course of this investigation, it was observed that as the steric bulk of the ligand increased, the solubility of the corresponding $[Tl(OR)]_n$ decreased (solubility of **1** > **2** > **3** ≈ **4** > **5** > **6**). Compounds **1** - **4** were soluble in hexanes, approaching approximate molarities of miscible, 3, 0.3, and 0.3, respectively. Compound **5** was only slightly soluble in toluene and **6** was insoluble in toluene and only slightly soluble in THF. Although steric factors often play a role in determining the solubility of metal alkoxides, the trend is generally the reverse of that observed for this series of compounds (i.e., typically, the more sterically demanding ligands yield smaller, more soluble compounds). In a previous study, A. G. Lee reported that a small decrease in the pKa of the aryl-alcohol resulted in an increase in the ionic character of the corresponding $[Tl(OR)]_n$.[21] Since an increase in ionic character typically results in a decrease in solubility in non-polar solvents, this explanation was invoked more generally to explain the solubility trend observed for **1** - **6**. To verify the increased ionic character of the less soluble compounds (**5** and **6**), crystal structure determinations and solution data were collected. The results of those studies are presented below.

Solid State Structures. Table 1 summarizes the collection parameters for **4** – **6**. Table 2 lists selected distances and angles for **4** – **6**. Due to the similarities of the two independent $[Tl(ONep)]_4$ molecules in the unit cell of **4**, only one set of metrical data are presented in Table 2 Full structural details are available in the Supporting Information section of this paper. Figures 1

- 3 show the thermal ellipsoid or ball and stick plots for **4** - **6** respectively. The solid state structures of **4** - **6** were the only $[Tl(OR)]_n$ species of which crystals suitable for single crystal X-ray diffraction were successfully grown. Several attempts were undertaken to structurally identify **2** and **3**; however, disorder in the crystals did not allow for the connectivity of the final complex to be identified.

Tl(OR) have been characterized by a host of analytical methods as tetrameric cubane compounds. However, only a partial structure of the methoxide derivative, $[Tl(OMe)]_4$, has been crystallographically determined.[22] Due to technical limitations, only the Tl atom positions could be refined and thus, the sole metrical data supplied for $[Tl(OMe)]_4$ were the Tl---Tl distances. Therefore, the structure of **4** is the first fully refined $[Tl\text{-}O]_4$ cubane cage. Two independent molecules were identified in the unit cell with significant disorder noted for the hydrocarbon groups of the ONep ligands. In agreement with literature reports, the Tl atoms in **4** are formally 3-coordinate, adopting a pseudo-T_d arrangement with the fourth site occupied by the stereochemically active lone pair. The distortion of the cube observed in **4** was predicted by Dahl, et. al., and described as a cube containing superimposed Tl and O tetrahedron with the oxygen tetrahedron being slightly smaller. This distortion gives rise to Tl-O-Tl angles slightly larger than 90° and O–Tl–O angles which are slightly smaller. The average Tl–O distance in **4** is 2.47 Å. A comparison of the OMe and ONep analogs reveals no significant change in the Tl---Tl distances at 3.84 and 3.76 Å respectively.

Figures 2 and 3 are the thermal ellipsoid plots of **5** and **6**, respectively. Both compounds, in contrast to other structurally identified Tl(OR), are one-dimensional polymers with a $[\text{-}Tl\text{-}O]_\infty$ backbone (each backbone oxygen originating from a phenoxide ligand). Only slight differences were observed in the metrical data of **5** and **6**. Since there are no close contacts between polymer

strands of either $[Tl(OAr)]_\infty$, each Tl atom in both compounds is two coordinate with one short (2.37 Å, **5**; 2.43 Å, **6**) and one long Tl-O distance (2.59, **5**; 2.59 Å, **6**). The geometry about each Tl is distorted trigonal planar due to the presence of a stereochemically active lone pair. The average Tl-O distance in **5** (2.48 Å) is just slightly shorter than the average for **6** (2.51 Å). The shorter metal-oxygen distance in both species is concurrent with a larger Tl-O-C angle (125.0° vs. 103.8° in **5**, 124.6° vs. 106.6° in **6**) suggesting possible π-donation to the metal center by the phenoxide oxygen. Along with the alternating short and long Tl-O distances, the chain incorporates alternating acute and obtuse angles (for **5**, O-Tl-O = 92.16°; Tl-O-Tl = 131.09°). This trend is also observed for the more sterically hindered **6**.

In contrast to **5** *and* **6**, the two Tl(OAr) complexes previously reported, $[Tl\{\mu\text{-}O(C_6H_4)\text{-}(C_6H_4OH)\}]_2$[23] and $[Tl(OC_6H_2\text{-}2,4,6\text{-}(CF_3)_3)]_2$[24], were shown to be dinuclear. The Tl metal centers in the dimers are supported by very different aromatic alcohols, but inhabit nearly identical coordination environments. The first complex, $[Tl\{\mu\text{-}O(C_6H_4)\text{-}(C_6H_4OH)\}]_2$, utililizes an aromatic diolate which acts as a monodentate ligand with a non-interacting hydroxyl group. For both of the aforementioned dinuclear compounds each Tl atom is necessarily bound to two bridging oxygens, thereby rendering the bonding analogous to that observed in **5** and **6.** It is not readily apparent why the polymer chain adopted by **5** and **6** would be preferred over discrete dimeric units as both contain 2-coordinate thallium centers supported by bridging oxygens. It is worth noting that, while both **5** and **6** were exposed to strong Lewis-basic solvents during crystallization, no metal–solvent interactions were observed in the solid state structures.

Solution State. In order to determine if the solid state structures of **4** – **6** are retained in solution, ^1H and ^{13}C solution NMR experiments were undertaken and revealed only a single set

of resonances for each compound. Due to the high molecular symmetry of the solid state structures of **4 - 6**, only a single set of peaks is expected for the intact species. However, their possible dynamic solution behavior cannot be ruled out and may also result in a single ligand environment. Fortunately, due to the natural occurrence of two spin active Tl isotopes (^{203}Tl and ^{205}Tl) and their high sensitivity, Tl---Tl splitting may be used to elucidate solution structure where ^{1}H and ^{13}C NMR fail. ^{205}Tl was one of the first nuclides investigated by NMR as it is the third most receptive I = 1/2 nuclide.[25,26] In principle, fine structure produced by Tl---Tl coupling can be very complex because both ^{205}Tl and ^{203}Tl are spin I = 1/2 nuclei with a natural abundance of 70.5 % and 29.5 %, respectively. Previous solution studies on Tl(OR) concluded that these species were tetrameric based on the observed intensity ratios from Tl-Tl coupling in ^{205}Tl NMR (even though only 3 of the expected 7 lines were observed).[13]

Shown in Figure 4 are the observed spectra for the solution ^{203}Tl NMR of **1 - 4**. The analogous observed spectra for the ^{205}Tl NMR are shown in Figure 5. Figure 6 contains the simulated spectra and intensity ratios for ^{203}Tl and ^{205}Tl NMR of $[Tl(OR)]_4$ in which the splitting is the result of Tl---Tl scalar coupling in a species containing 2, 3, or 4 equivalent metal centers. Table 3 lists the observed and expected intensity ratios for the ^{203}Tl NMR of compounds **1 – 4**. The observation of seven line patterns verifies that the tetranuclear species isolated in the solid state (*vide infra*) must also be present in solution. This seven-line pattern is actually the superposition of a singlet (all one isotope – the resonating nuclide), doublet (one non-resonating nuclide), triplet (2 non-resonating nuclides), and quartet (3 non-resonating nuclides). Furthermore, since the observed intensity ratios are in good agreement with those expected for a tetranuclear species, it must be the major aggregate in solution. The observance of Tl---Tl coupling in **1 – 4** establishes an upper limit for fluxional processes that may be occurring (<<

$^2J_{203\text{-}205} \approx 2.5$ kHz). In contrast, the ^{203,205}Tl NMR spectra of **5** and **6** reveal a singlet for each compound. The single ^{203,205}Tl resonance is consistent with either the formation of a monometallic complex in solution, or the presence of a fluxional process involving a dissociation / association equilibrium. In contrast to **1 – 4**, the lack of Tl---Tl coupling establishes a lower limit to possible fluxional process ($>> {}^2J_{203\text{-}205} \approx 2.5$ kHz).

As discussed previously, it has been observed that a decrease in the pKa of the ligand alcohol results in an increase in the ionic character of the resulting Tl(OR).[21] The previous observation was made for the case of small changes in pKa's for a number of Tl(OAr), but the current work suggests that it may be more generally applicable. An increase in ionic character typically results in a decrease in solubility in non-polar solvents. The ^{205}Tl chemical shifts of **1 – 6** suggest a general trend wherein an increase in ionic nature and decrease in alcohol pKa also correlates to a downfield shift of the corresponding resonance. While the solubility trend was not strictly followed for the aliphatic alcohols, the large pKa change from aliphatic to aromatic was commiserate with a significant solubility difference.

This general chemical shift trend was also observed in the solid state ^{205}Tl NMR of **2 – 6**. Table 4 contains the solution and solid state ^{205}Tl chemical shift values of **1 – 6** and the pKa's[27-29] of their corresponding alcohols. This data is presented graphically in Figure 7 and, while there are minor deviations, the general trend where an increase in ionic character effects a downfield chemical shift was recorded for both the solid state and solution data. Chemical shift values for **5** are not included in Figure 7 as they were ambiguous and experiments to clarify these results are underway.

The dependence of the ^{205}Tl chemical shift on both solvent and concentration has been reported for numerous Tl(I) complexes.[25,30,31] This characteristic has even been exploited as a

means of establishing solvent donor numbers.[32,33] The Tl chemical shift dependence upon concentration is generally less significant as evidenced by an order of magnitude variation in concentrations for both **1** and **5** which resulted in only slight chemical shift differences (< 20 ppm). For the cubane structure of **4**, the seven-line ^{203}Tl resonance was found to exist independent of the solvent utilized for dissolution and observed at very similar frequencies (< 20 ppm difference). This indicates that the Tl cations of the cubane structures are almost completely protected from outside influences (i.e., no coordination of solvent is possible for the cubane structure). In the case of **5**, a chemical shift difference was observed when the compound was dissolved in solvents of differing donor ability (1989 ppm in toluene and 1916 ppm in pyridine). Because the ^{205}Tl resonance for dilute $Tl(NO_3)$ in pyridine appears at ~800 ppm[32], the upfield shift for the pyridine sample is expected if any solvent / metal interaction is present. While the chemical shift is obviously still governed by the Tl-OAr interaction, the slight change indicates that the Tl^+ in **5** interacts with strong Lewis-basic solvents. Both **5** and **6** are much more soluble in polar solvents than in nonpolar solvents while the opposite trend was observed for **4**. The larger solvent dependence on chemical shift and increased solubility in polar solvents support the view of Tl(OAr) as generally more ionic in comparison to their alkyl counterparts. The dissociation / association equilibria expected for ionic species may also explain the loss of Tl---Tl coupling in **5** and **6**.

Summary and Conclusion.

We have successfully synthesized and characterized a series of $[Tl(OR)]_n$ compounds. While the simple alkoxides adopt a cubane structure (**1 – 4**), the bulky aryloxides form novel one-dimensional polymers (**5, 6**). The solid state structures were also investigated using ^{205}Tl

MAS NMR spectroscopy and found to be consistent with the solid state structures. ^{203,205}Tl solution NMR of **1** - **4** confirmed that these samples maintained their cubane structures in solution, consistent with literature reports, and were unaffected by the choice of solvent. In contrast, **5** and **6** are considerable more ionic appearing to be fluxional in solution and, thus, more susceptable to solvent variations. Chemical shift values from the ^{203,205}Tl solution NMR of **1** – **6** follow a general trend, wherein an increase in the metal ionic character correlates to a downfield shift. The degree of ionic character can be predicted, and increased covalency of the Tl(OR) complex can be imposed by utilizing stronger electron donating alkoxides (increased pKa of the parent alcohol).

Acknowledgements. For support of this research, the authors would like to thank the United States Department of Energy under contract DE-AC04-94AL85000. Sandia is a multi-program laboratory operated by Sandia Corporation, a Lockheed Martin Company, for the United States Department of Energy. The authors thank Karen Ann Smith for continued access to the ASX300 spectrometer and Martine Ziliox for loan of the solid state Tl preamplifier.

Supporting Information Available. Full summaries of X-ray diffraction data, listings of atomic coordinates and anisotropic thermal parameters, hydrogen atom positions, and full bond distances and angles; listing of observed and calculated structure factors. Ordering information is given on any current masthead page.

References

1. Caulton, K. G.; Hubert-Pfalzgraf, L. G. *Chem. Rev.* **1990**, *90*, 969.

2. Bradley, D. C. *Chem. Rev.* **1989**, *89*, 1317.

3. Chandler, C. D.; Roger, C.; Hampden-Smith, M. J. *Chem. Rev.* **1993**, *93*, 1205.

4. Bradley, D. C.; Mehrotra, R. C.; Gaur, D. P. *Metal Alkoxides*; Academic Press: New York, 1978.

5. Veith, M.; Mathur, S.; Mathur, C. *Polyhedron* **1998**, *17*, 1005.

6. Hampden-Smith, M. J.; Williams, D. S.; Rheingold, A. L. *Inorg. Chem.* **1990**, *29*, 4076.

7. Mehrotra, R. C. *J. Chem. Soc. A* **1967**, 1026.

8. Boyle, T. J.; Bradley, D. C.; Hampden-Smith, M. J.; Patel, A.; Ziller, J. W. *Inorg. Chem.* **1995**, *34*, 5893.

9. Boyle, T. J.; Alam, T. M.; Tafoya, C. J.; Mechenbier, E. R.; Ziller, J. W. *Inorg. Chem.* **1999**, *38*, 2422.

10. Gulliver, E. A.; Garvey, J. W.; Wark, T. A.; Hampden-Smith, M. J.; Datye, A. *J. Am. Ceram. Soc.* **1991**, *74*, 1091.

11. Veith, M.; Kunze, K. *Angew. Chem. Int. Ed. Engl.* **1991**, *30*, 95.

12. Lamy, A. *Ann. Chim. Phys.* **1863**, *67*, 365.

13. Burke, P. J.; Matthews, R. W.; Gillies, D. G. *J. Chem Soc., Dalton Trans.* **1980**, 1439.

14. Maroni, V. A.; Spiro, T., G. *Inorg. Chem.* **1968**, *7*.

15. SMART Version 5.054, **1998**, Bruker Analytical X-ray Systems, Inc., 6300 Enterprise Lane, Madison, Wisconson 53719.

16. SAINT Version 6.01, **1998**, Bruker Analytical X-ray Systems, Inc., Madison, Wisconsin 53719.

17. SADABS, first release, George Sheldrick, University of Göttingen, Germany.

18. SHELXTL/NT Version 5.10, **1998**, Bruker Analytical X-ray Instruments, Inc., Madison, Wisconsin 53719.

19. XSHELL Version 3.0, **1997**, Bruker Analytical X-ray Systems, Inc., 6300 Enterprise Lane, Madison, WI 53719.

20. $R1 = \sigma\|F_o|-|F_c\|/\sigma|F_o|$. and $R2_w = \left[\Sigma\left[w(F_o^2 - F_c^2)^2\right]/\Sigma\left[w(F_o^2)^2\right]\right]^{1/2}$

21. Lee, A. G. *J. Chem. Soc. (A)* **1971**, 2007.

22. Dahl, L. F.; Davis, G. L.; Wampler, D. L.; West, R. *J. Inorg. Nucl. Chem.* **1962**, *24*, 357.

23. Elhadad, A. A.; Kickham, J. E.; Loeb, S. J.; Taricani, L.; Tuck, D. G. *Inorg. Chem.* **1995**, *34*, 120.

24. Roesky, H. W.; Scholz, M.; Noltemeyer, M.; Edelmann, F. T. *Inorg. Chem.* **1989**, *28*, 3829.

25. Hinton, J. F. *Mag. Res. Chem.* **1987**, *25*, 659.

26. Bloembergen, N.; Rowland, T. J. *Acta Metall.* **1953**, *1*, 731.

27. Reeve, W.; Erikson, C. M.; Aluotto, P. F. *Can. J. Chem.* **1979**, *57*, 2747.

28. Takahashi, S.; Cohen, L. A.; Miller, H. K.; Peake, E. G. *J. Org. Chem.* **1971**, *36*, 1205.

29. See: Bordwell, F. G.; McCallum, R. J.; Olmstead, W. N. *J. Org. Chem.* **1984**, *49*, 1424; and references therein.

30. Srivanavit, C.; Zink, J. I.; Dechter, J. J. *J. Am. Chem. Soc.* **1977**, *99*, 5876.

31. Siddique, R. M.; Winfield, J. M. *J. Fluorine Chem.* **1988**, *40*, 71.

32. Briggs, R. W.; Hinton, J. F. *J. Solution Chem.* **1977**, *6*, 827.

33. Briggs, R. W.; Hinton, J. F. *J. Solution Chem.* **1979**, *8*, 519.

List of Tables

List of Figures

Table 1: Data collection parameters for **4**, **5**, and **6**.

Compound	**4**	**5**	**6**
Chemical formula	$C_{20}H_{44}O_4Tl_4$	C_8H_9OTl	$C_{12}H_{17}OTl$
Formula weight	1166.03	325.52	381.648
Temperature (K)	168	168	168
space group	cubic	hexagonal	monoclinic
crystal system	P-43n	R3c	$P2_1/c$
a (Å)	18.139(1)	25.269(2)	9.510(2)
b (Å)	---	25.269(2)	6.600(1)
c (Å)	---	6.632(1)	20.268(4)
α (°)	---	---	---
β (°)	---	---	102.591(2)
γ (°)	---	---	---
V (Å^3)	5968.2	3667.1	1241.5
Z	8	18	4
D_{calcd}(mg/m^3)	2.595	2.653	---
μ (mm^{-1})	21.55	19.80	25.952
R1[a] (%)	6.82	2.21	6.84
wR2[b] (%) [I>2σ(I)]	20.15	5.14	18.88
R1[a] (%, all data)	10.49	2.35	8.08
wR2[b] (%, all data)	22.15	5.20	20.15

Table 2: Selected distances and angles for **4**, **5**, and **6**.

Distances (Å)	**4**		**5**		**6**	
Tl---Tl	Tl(1A)---Tl(1B)	3.766(3)	Tl(1A)---Tl(1B)	4.516(3)	Tl(1A)---Tl(1B)	4.513(5)
	Tl(1A)---Tl(1C)	3.750(2)				
	Tl(1A)---Tl(1D)	3.750(2)				
Tl-μ-O	Tl(1A)-O(1A)	2.463(15)	Tl(1A)-O(1A)	2.589(4)	Tl(1A)-O(1A)	2.588(7)
	Tl(1A)-O(1AA)	2.464(17)	Tl(1A)-O(1AA)	2.372(4)	Tl(1A)-O(1AA)	2.429(7)
	Tl(1A)-O(1BA)	2.475(17)				
Angles (°)						
Tl-O-Tl	Tl(1A)-O(1A)-Tl(1B)	99.7(6)	Tl(1A)-O(1)-Tl(1B)	131.09(18)	Tl(1A)-O(1AA)-Tl(1B)	128.1(3)
	Tl(1A)-O(1A)-Tl(1D)	98.8(6)				
	Tl(1B)-O(1A)-Tl(1D)	98.8(6)				
O-Tl-O	O(1A)-Tl(1A)-O(1AA)	79.7(6)	O(1A)-Tl(1A)-O(1AA)	92.16(8)	O(1A)-Tl(1A)-O(1AA)	92.83(13)
	O(1A)-Tl(1A)-O(1BA)	80.3(6)				
	O(1AA)-Tl(1A)-O(1BA)	80.3(6)				
Tl-O-C	Tl(1A)-O(1)-C(1)	103.5(15)	Tl(1A)-O(1A)-C(1A)	103.8(4)	Tl(1B)-O(1AA)-C(1AA)	106.6(5)
	Tl(1B)-O(1)-C(1)	150.5(9)	Tl(1A)-O(1AA)-C(1AA)	125.0(4)	Tl(1A)-O(1AA)-C(1AA)	124.6(6)
	Tl(1D)-O(1)-C(1)	95.5(13)				

Table 3: Calculated and observed intensity ratios for ^{205}Tl and ^{203}Tl NMR of thallium alkoxides

Compound		**Septet Intensity Ratio**												
	calculated	**1**	**:**	**2.6**	**:**	**5.2**	**:**	**5.8**	**:**	**5.2**	**:**	**2.6**	**:**	**1**
1	**observed**	1	:	2.7	:	5.4	:	6.0	:	5.4	:	2.7	:	1
2		1	:	2.9		5.9	:	6.0	:	5.9	:	2.9	:	1
3		1	:	2.8	:	5.7	:	6.4	:	5.7	:	2.8	:	1
4		1	:	2.7	:	6.0	:	6.8	:	6.0	:	2.7	:	1

Table 4: Chemical shift values for ^{205}Tl NMR of **1 – 6** and pKa's of corresponding alcohols.

Compound	δ (ppm)		pKa of parent alcohol
	Solution ($J_{203-205}$, kHz)	Solid State	
1	2914 (2.54)	----	15.9 [27]
2	3067 (2.57)	3184	16.5 [27]
3	3287 (2.35)	4340	16.5 [27]
4	2561 (2.58)	3437	16 [28]
5	1999	3150, 2120, 1880	10-11 [29]
6	1850	1570	10-11 [29]

Figure 1

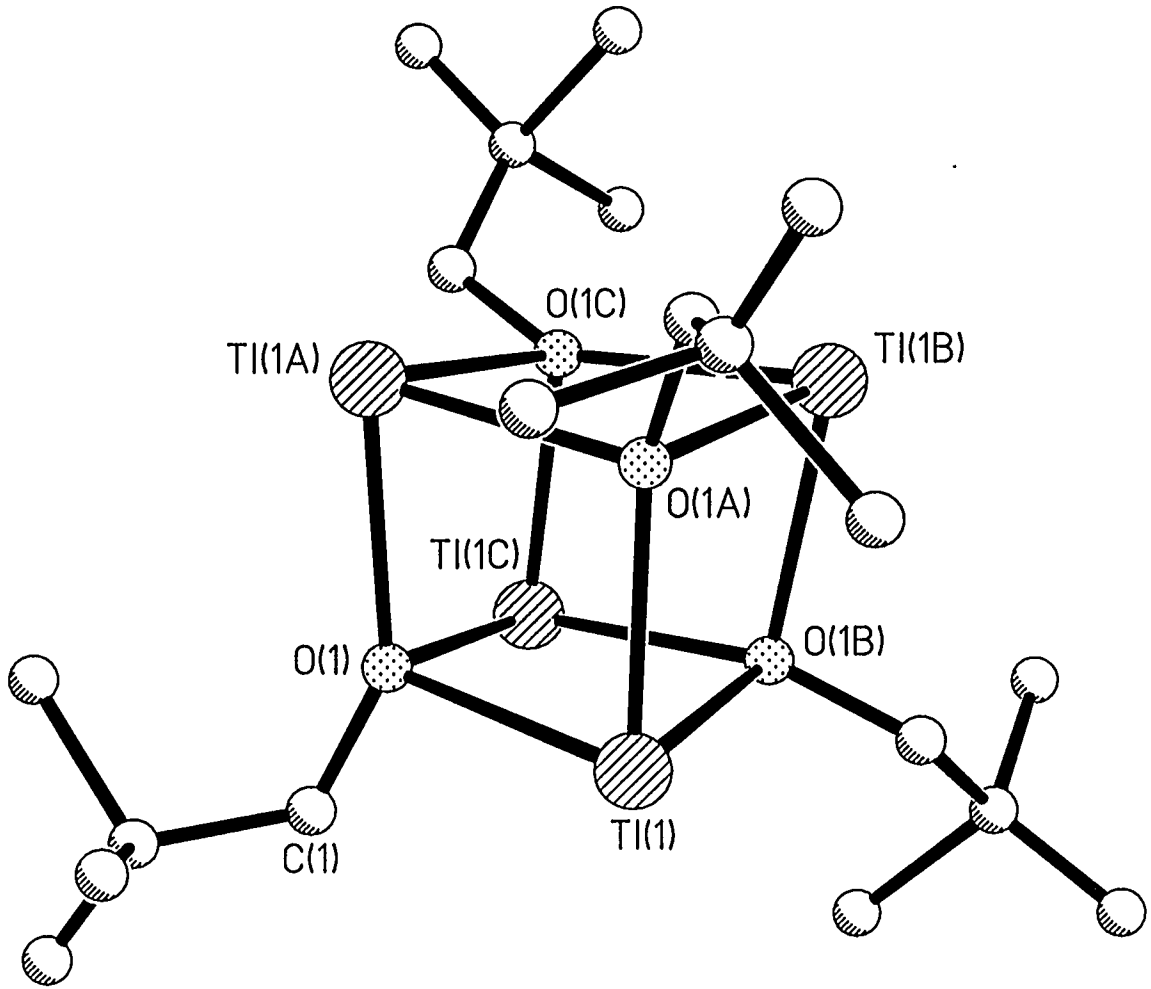

figure 2

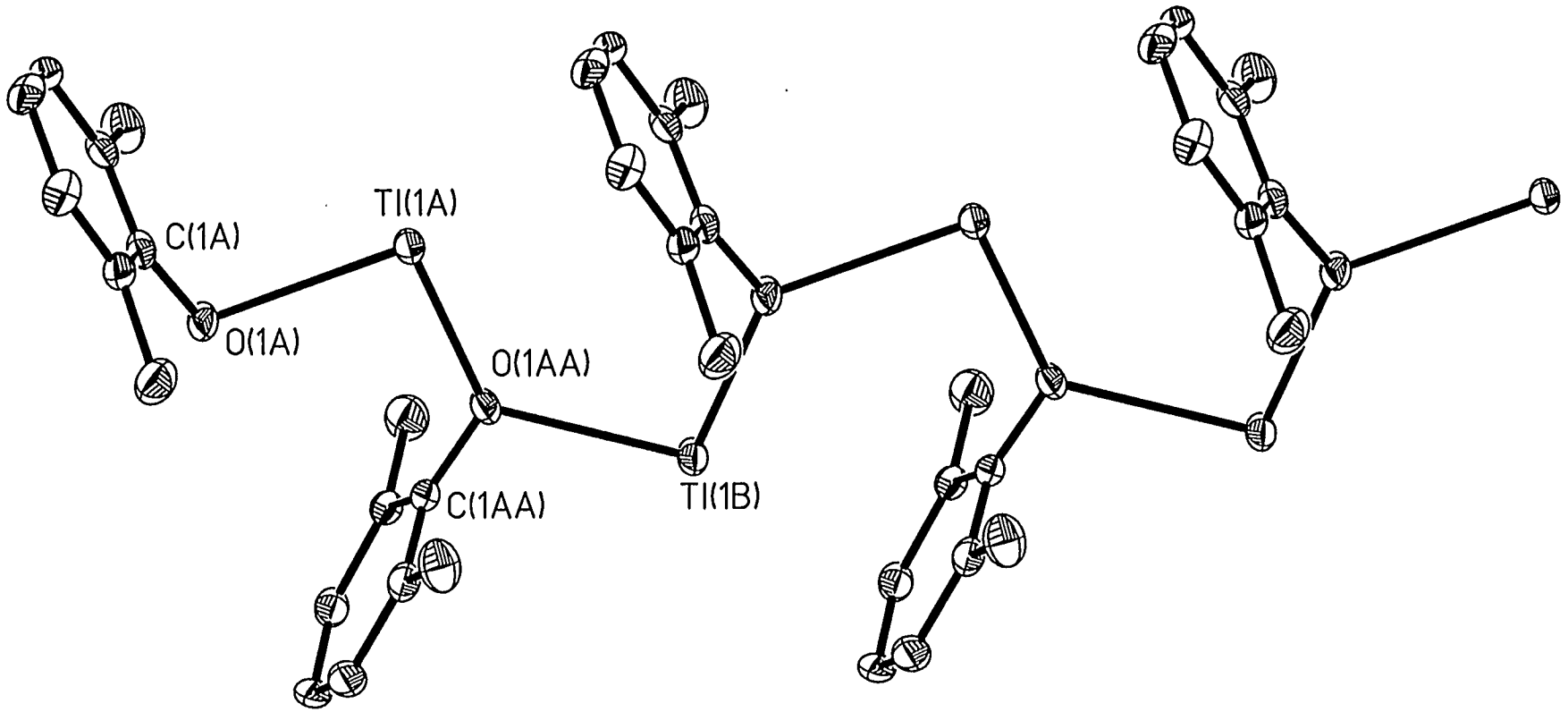

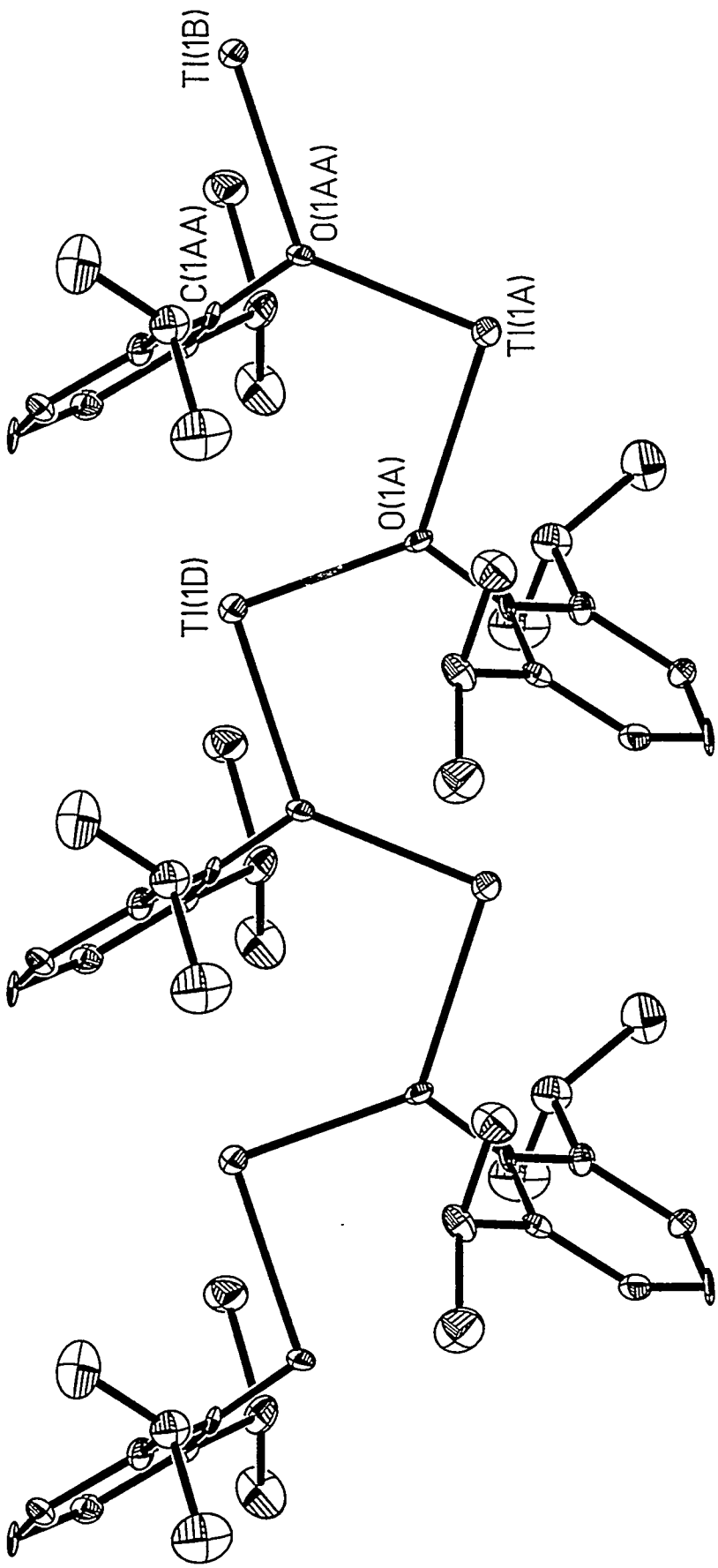

figure 3

Figure 4

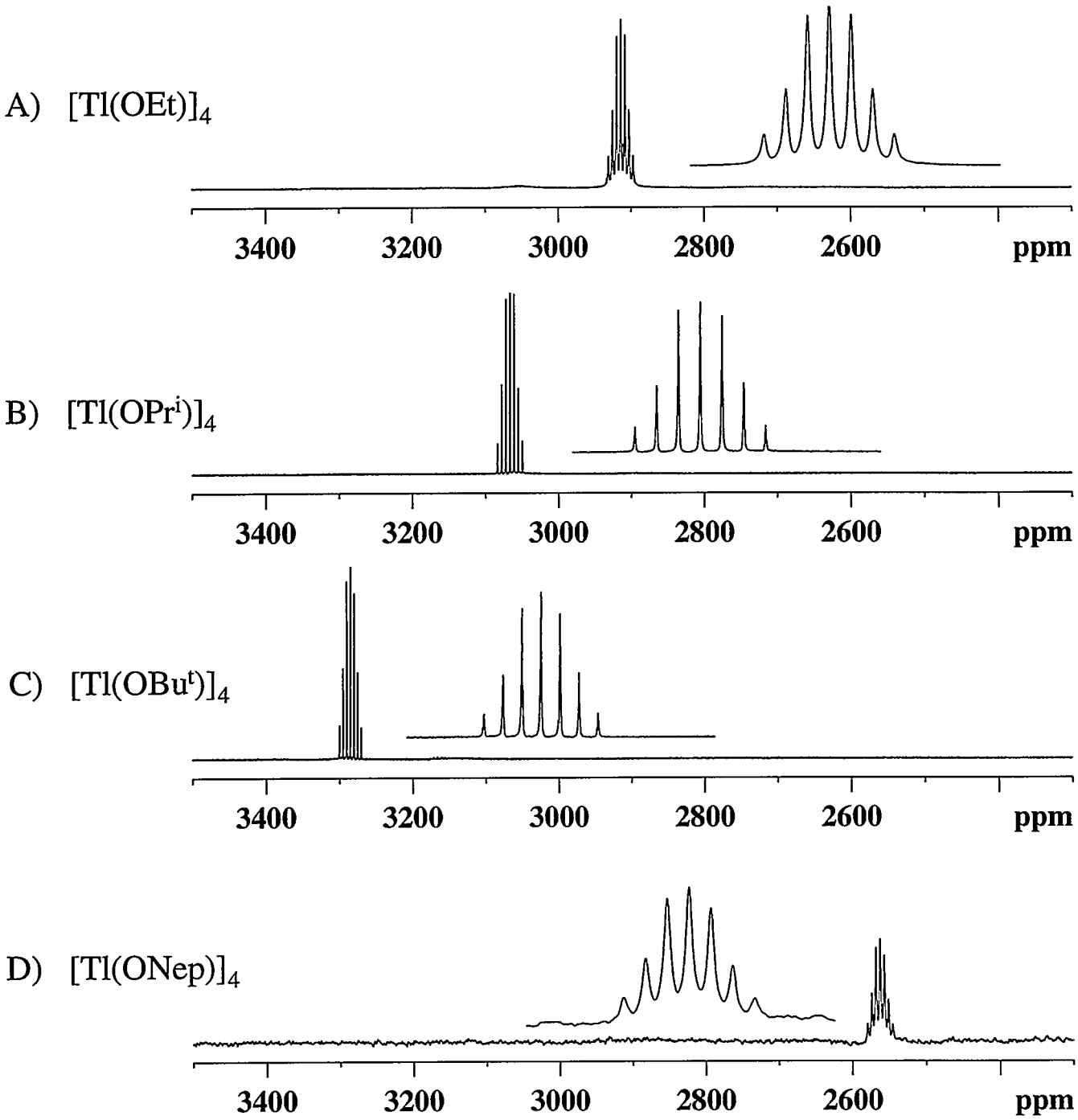
A) [Tl(OEt)]4
3400
3200
3000
2800
2600
ppm
B) [Tl(OPr^i)]4
3400
3200
3000
2800
2600
ppm
C) [Tl(OBu^t)]4
3400
3200
3000
2800
2600
ppm
D) [Tl(ONep)]4
3400
3200
3000
2800
2600
ppm

Figure 5

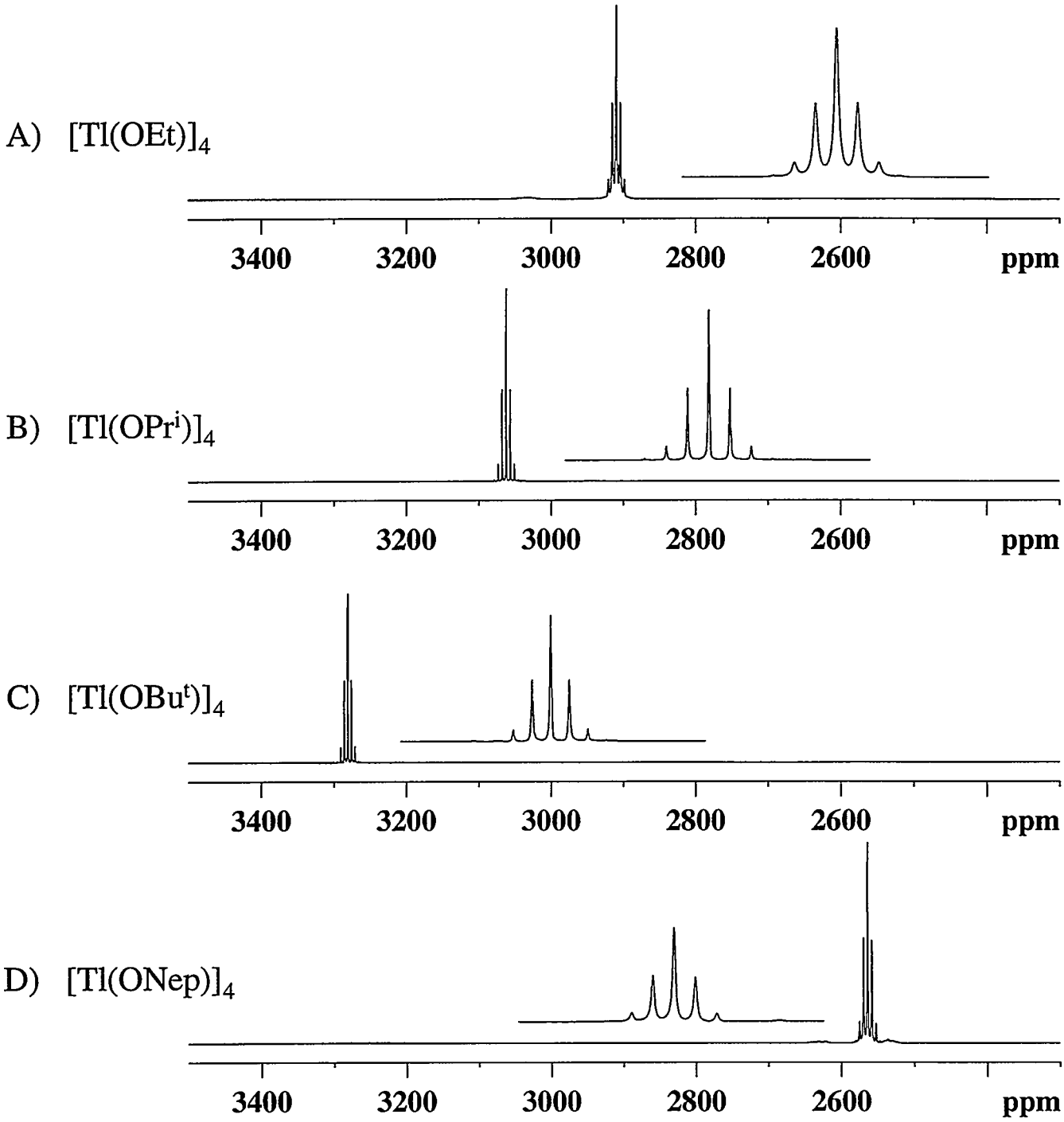
A) [Tl(OEt)]4
3400
3200
3000
2800
2600
ppm
B) [Tl(OPri)]4
3400
3200
3000
2800
2600
ppm
C) [Tl(OBut)]4
3400
3200
3000
2800
2600
ppm
D) [Tl(ONep)]4
3400
3200
3000
2800
2600
ppm

Figure 6

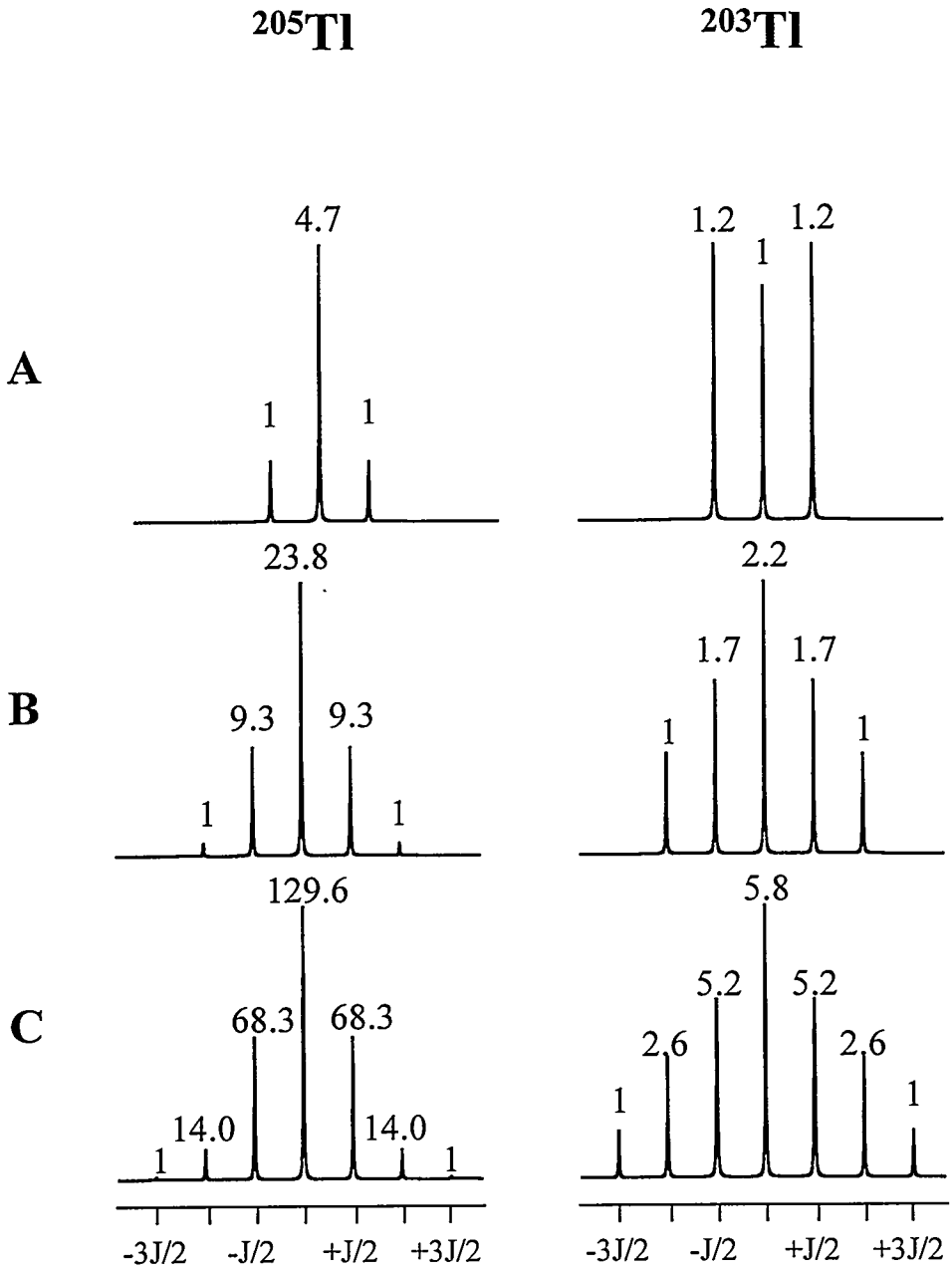
205Tl
203Tl
A
4.7
1
1
1.2
1
1.2
B
23.8
9.3
9.3
1
1
2.2
1.7
1.7
1
1
C
129.6
68.3
68.3
14.0
14.0
1
1
5.8
5.2
5.2
2.6
2.6
1
1
-3J/2
-J/2
+J/2
+3J/2
-3J/2
-J/2
+J/2
+3J/2

Figure 7

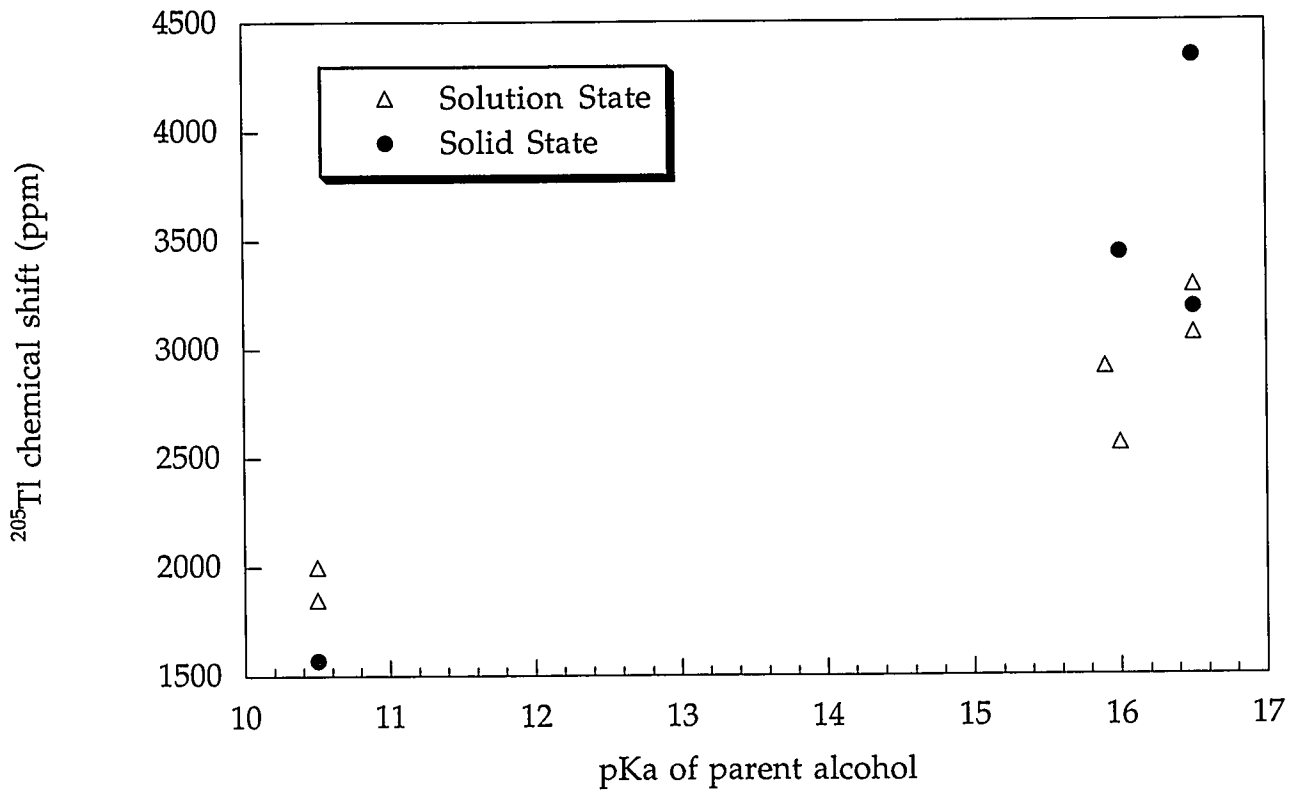
4500
4000
3500
3000
2500
2000
1500
10
11
12
13
14
15
16
17
Solution State
Solid State
^{205}Tl chemical shift (ppm)
pKa of parent alcohol